

Supplementary figure 1. Schematized experimental timelines. **A:** Timeline (in months) for monkey experiments showing sequence of events, including MPTP intoxication, stabilization period of parkinsonian symptoms, chronic vehicle or L-dopa treatment, intracranial virus injection, post-viral pharmacological monitoring and termination. Upward pointing arrowheads symbolizes the repeated behavioural observations. **B:** Timeline (in days) for rat experiments showing sequence of events, including unilateral 6-OHDA lesion, recovery period, stepping test, initiation of daily L-dopa/benserazide injections (6 mg/kg/15mg/kg i.p.), period of every other day injections (intermit), intracranial virus injection or intrastriatal peptide administration follow-up behavioural experiments and termination. Upward pointing arrowheads symbolizes the repeated behavioural observations. **C:** Timeline (in days) for primary striatal culture experiments showing sequence of events, including culture preparation from embryonic rats, plasmid transfection and Quantum-Dot / immunochemical experiments.

Supplementary figure 2. SAP97 levels. **A:** Representative western blot using anti-SAP97 (Enzo Life Sciences-ADI-VAM-PS005, 1/1000) and tubulin antibodies from putamen extracts of the different experimental monkey groups (n=6 animals per group) that were prepared as depicted in supplemental figure 1. Bar graph represents the relative intensity of the SAP97/tubulin ratio and indicates that endogenous SAP97 is significantly increased in the putamen of control monkeys exposed to chronic L-dopa (★ vs. controls; , $p < 0.05$) but not in MPTP and MPTP exposed to L-dopa monkeys (3 independent experiments). **B:** Detection of SAP97 (Enzo Life Sciences-ADI-

VAM-PS005, 1/1000) by Western blot using anti-SAP97 antibody in striata extracts from animals which behaviour is shown in Figure 2B. Both lesioned (L) and unlesioned sides (UL) are illustrated. Graph shows the relative level of SAP97 in the different experimental groups (from 3 independent experiments). shPSD did not affect the expression of SAP97 in comparison with mock group. ★ indicates a significant difference of SAP97 levels in comparison with mock group ($p < 0.05$).

Supplementary figure 3. Extent and pattern of LV-mediated transfection in the rat DA-depleted striatum. Representative low (A) and high (B) magnification photomicrograph of striatal sections around the injection site infected with the different LVs. Brain sections were immunostained with an anti-GFP antibody (green) to label LV-mediated transgene expression and PSD-95 (red). Fluorescence was visualized by direct (A) and confocal (B) microscopy. Mock animals displayed a clear co-immunolabelling in medium spiny-like neurons of the dorsal striatum. Increased PSD-95 levels are clearly visible in PSD-95-treated animals while shPSD group shows a dramatic reduction in PSD-95-immunolabelling in the GFP-immunopositive medium spiny-like neurons.

Supplementary figure 4. 3-dimensional reconstruction of GFP immunostaining. Sequential mapping (Mercator, Explora Nova, La Rochelle, France) on acetylcholinesterase stained sections (1 30 μm -thick section every 6th sections) allowed to define both the area of GFP immunostaining (green) and the boundaries of the striatum (red) within the limits of the brain (blue). 3-D reconstruction was achieved with Map 3D software (Explora Nova).

Supplementary figure 5. D1-CT peptide interacts with PSD-95. Western blot with anti-PSD-95 of protein extracts from rat or monkey brain tissue as well as HEK293 cells expressing PSD-95 or PSD-95-GFP before (input) or after pull down by immobilized active D1-CT or control D1-SCR peptides. Images are representative of 6 independent experiments.

Supplementary figure 6. Effect of PSD-95 levels upon DA and glutamate receptors localization in the rat striatal medium spiny neurons. In set 2 (Figure 2B), double immunofluorescence was conducted for GFP (green) and D1R, D2R, mGluR5, GluN2A and GluN2B (all in red).

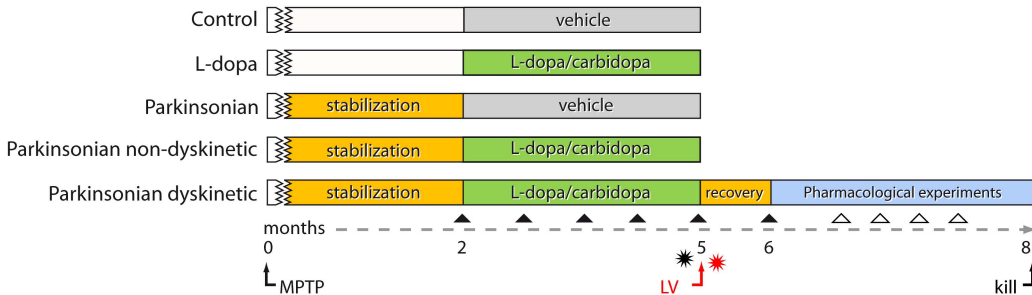
Vibratome-cut (Leica, VT1000S) 60 μm -thick striatal sections were collected in PBS (0.01 M phosphate, pH 7.4). Sections were equilibrated in a cryoprotectant solution (0.05 M PB, pH 7.4, containing 25% sucrose and 10% glycerol), freeze-thawed and stored in PBS with 0.03% sodium azide. D1R, D2R, mGluR5, GluN2A and GluN2B were detected by fluorescent

immunohistochemistry using different antibodies: D1R, monoclonal antibody raised in rat against a 97 aa sequence corresponding to the C terminal of the human D1R (Sigma); D2R, an affinity-purified rabbit polyclonal antiserum directed against a 28 aa sequence from the human D2receptor within the third cytoplasmic loop (Millipore Corporation); mGluR5, an affinity-purified rabbit polyclonal antiserum directed against specific peptide from rat mGluR5 (Millipore Corporation); GluN2A, an purified rabbit polyclonal antiserum directed against peptide GHSHDVTTERELRN(C) corresponding to amino acid residues 41-53 (extracellular N-terminal domain) of rat NMDAR2A (Alomone Labs); GluN2B, monoclonal antibody raised in mouse against fusion protein amino acids 20-271 (extracellular N-terminal domain) of rat GluN2B (UC Davis/NIH NeuroMab Facility). The antibodies were detected using the tyramide signal amplification system (NEN). Sections were incubated in 0.5% blocking reagent (TSA indirect kit, NEN) containing 0.05% tween 20 for 45 min and then in D1R (1:10000) or D2R (1:3000) or mGluR5 (1:4000) or GluN2A (1:4000) or GluN2B (1:2000) antibody supplemented with 1% normal goat serum or normal donkey serum overnight at room temperature. Sections were then incubated for 90 min in biotinylated goat anti- rat, goat anti-mouse or donkey anti-rabbit IgG (1:200 in PBS, VWR) followed by streptavidin-horseradish peroxidase 1:100 in 0.5% blocking reagent (SA-HRP, TSA indirect kit, NEN) for 30 min. The sections were then PBS-washed and incubated for 7 min in biotinyl tyramide 1:100 in amplification diluent (TSA indirect kit, NEN). Sections were incubated with streptavidin Alexa Fluor 568 conjugate (1:1000 in 0.5% blocking reagent, Invitrogen) for 30 min. GFP labelling was directly detected by fluorescent microscopy. The sections were mounted on glass slides in vectashield (Vector Laboratories). Negative immunohistochemical controls demonstrated the absence of signal when omitting the first antibody.

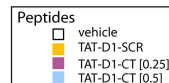
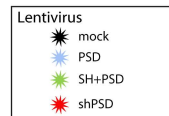
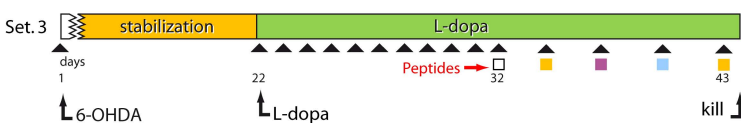
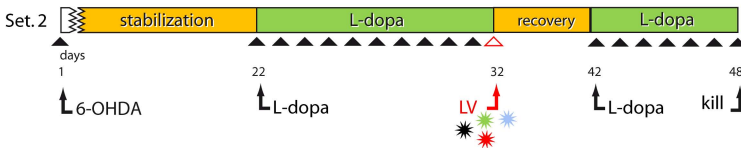
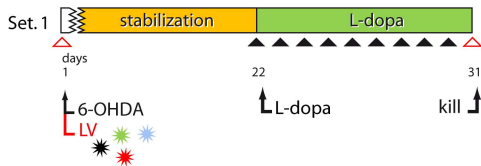
Supplementary figure 7. PSD-95 knockdown does not alter D1R or surface GluN2B-NMDAR content. Striatal cultured neurons transfected with shPSD-95-GFP were immunostained for PSD-95 (total), D1R (total), or GluN2B subunit (only surface). The staining intensity (arbitrary unit, a.u.) of these markers (red staining) was then compared between transfected (GFP detection, left panels) and neighbouring untransfected neurons (right panels). The PSD-95 intensity was significantly reduced in shPSD-95 neurons (untrans, n = 6 neurons, N = 59 dendritic fields; shPSD-95, n = 5 neurons, N = 31 dendritic fields, ★, p < 0.01; unpaired t test). The D1R (untrans, n = 6 neurons, N = 57 dendritic fields; shPSD-95, n = 6 neurons, N = 36 dendritic fields) or GluN2B subunit (untrans, n = 8 neurons, N = 61 dendritic fields; shPSD-95, n = 4 neurons, N = 34 dendritic fields) intensity was not significantly affected in shPSD-95 neurons.

Supplementary figure 8. TAT-D1-CT peptide does not alter GluN2A and GluN2B NMDAR localization in the rat striatal medium spiny neurons. Striatal cultured neurons exposed to vehicle, TAT-D1-CT (5 μ M for 10 min) or TAT-D1-SCR (5 μ M for 10 min) were then immunostained for GluN2A (left column) or GluN2B subunits (right column). GluN2A and GluN2B were detected by fluorescent immunohistochemistry using antibodies raised against extracellular epitopes : GluN2A, purified rabbit polyclonal antiserum directed against peptide GHSHDVTERELRN(C) corresponding to amino acid residues 41-53 (extracellular, N- terminal) of rat NMDAR2A (1:150, Alomone Labs); GluN2B, rabbit polyclonal antibody raised against peptide (C)NTHEKRIYQSNMLNR corresponding to amino acid residues 323-337 (extracellular, N-terminal) of rat NMDAR2B (1:150; Alomone Labs). For GluN2A, cultures were fixed with a 37°C pre-warmed mixture of 4% paraformaldehyde in 0.1 M PB (pH 7.4) for 20 min, rinsed three times in PBS and permeabilized with 0.3% Triton X-100 in PBS for 30 sec at room temperature. Coverslips were then incubated in GluN2A antibody for 30 min at 37°C, PBS-washed and then incubated with Alexa 568-conjugated goat anti-rabbit IgG (1:500, Molecular Probes, Invitrogen) for 1h at room temperature. For GluN2B immunostaining, cultured neurons were incubated with primary antibody at 37 °C for 30 min in culture medium. Neurons were then fixed with 4% PFA for 15 min, washed, and incubated with Alexa 568-conjugated goat anti-rabbit IgG (1:500, Molecular Probes, Invitrogen) for 1h at room temperature. The staining intensity of these markers (red staining) was fully comparable across experimental conditions both at cell body and neurite levels (magnified inset in each panel).

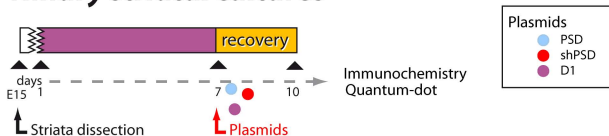
A. Monkey experiments

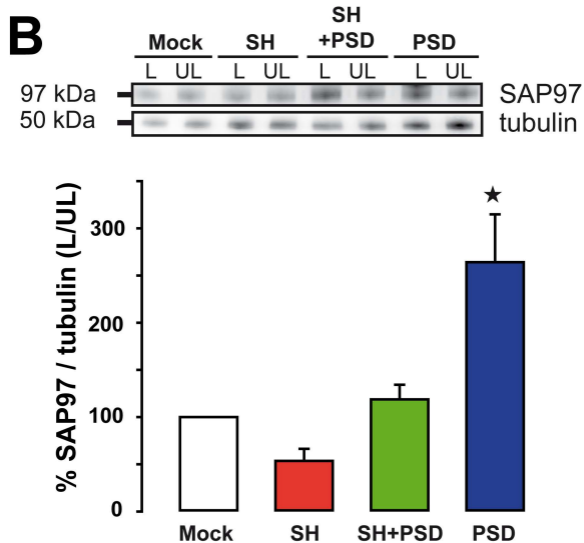
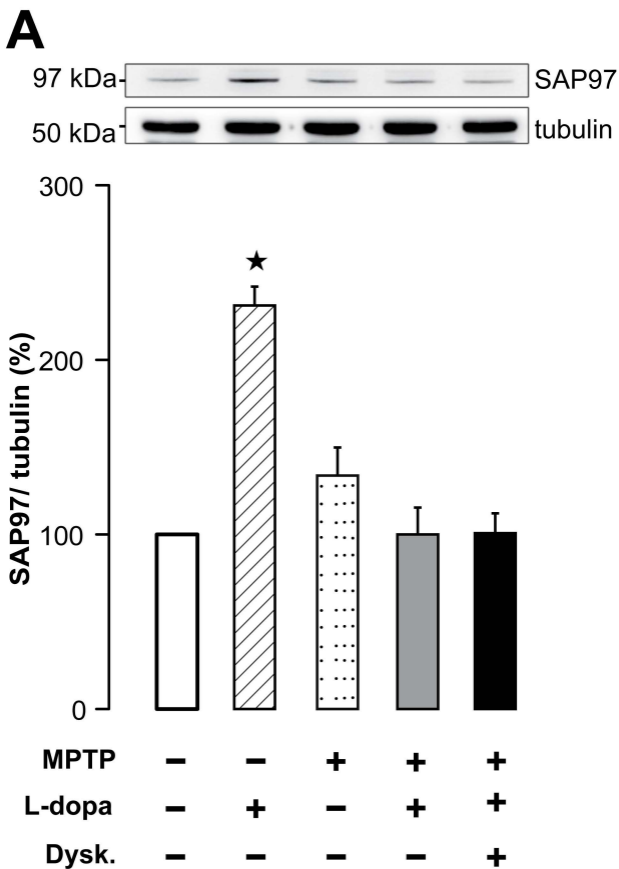


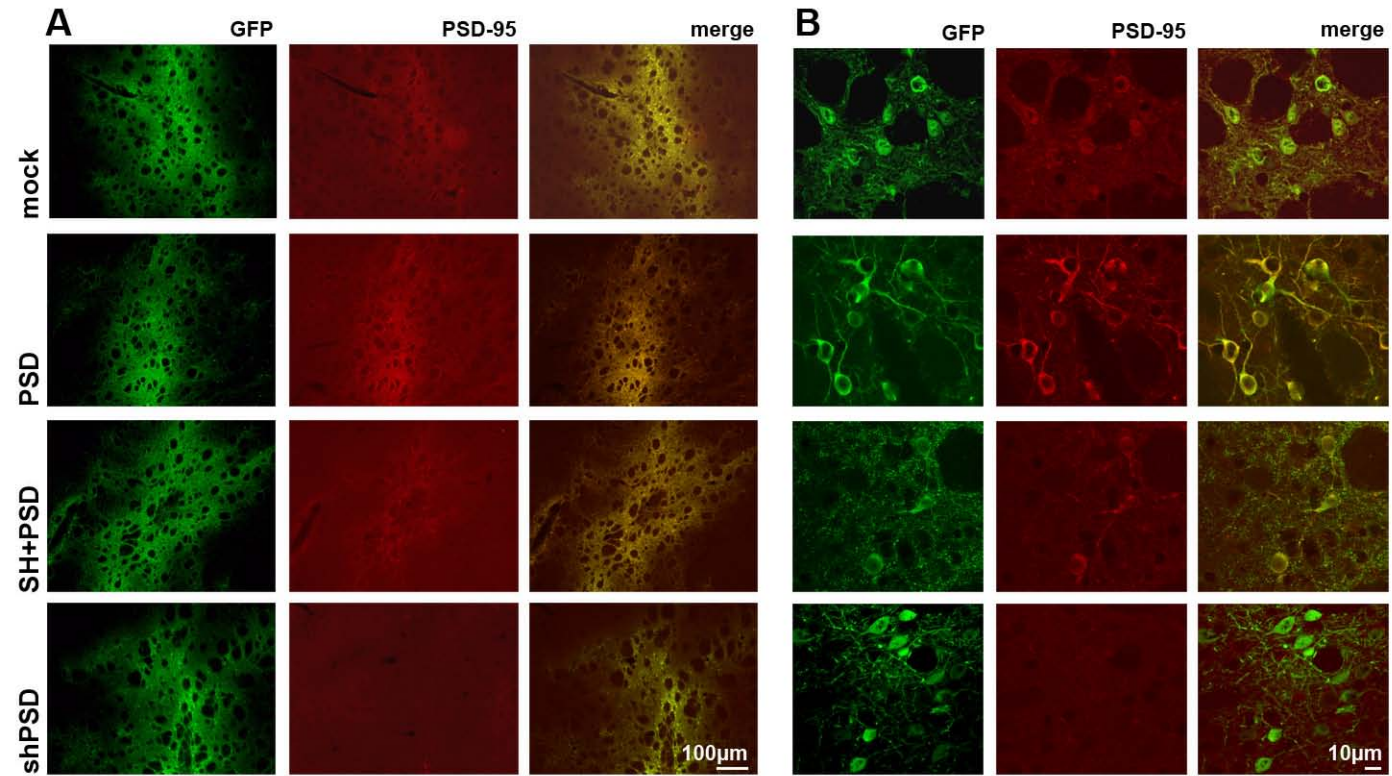
B. Rat experiments



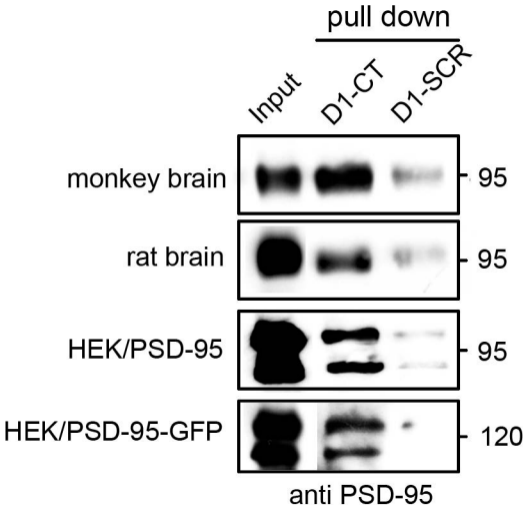
C. Primary striatal cultures

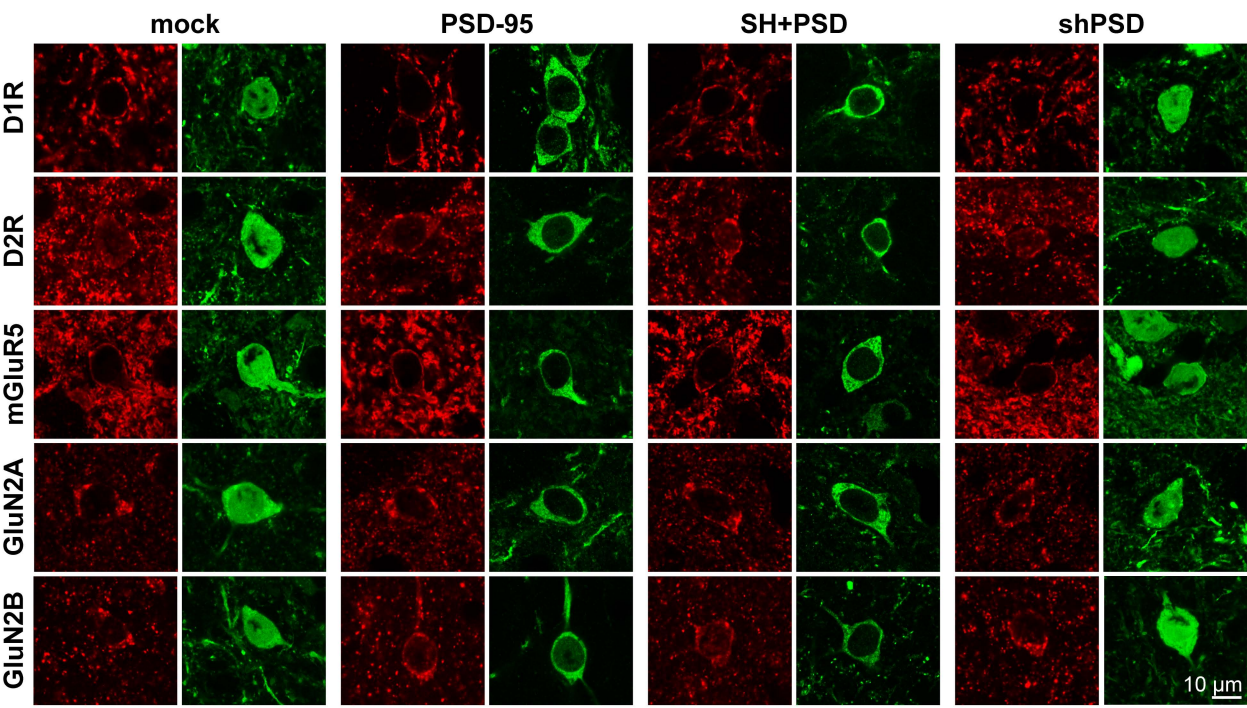




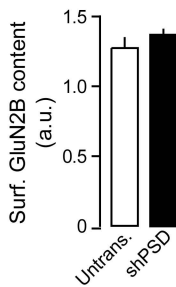
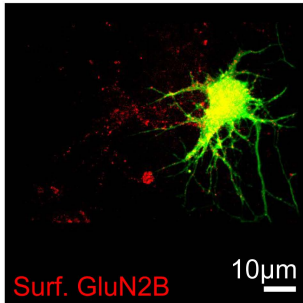
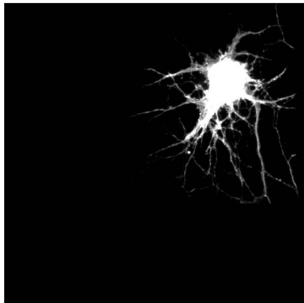
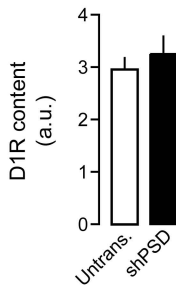
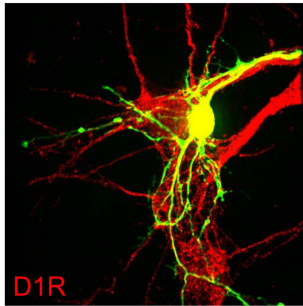
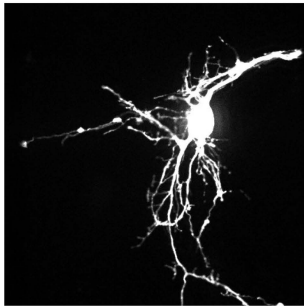
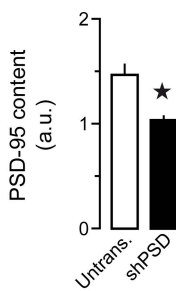
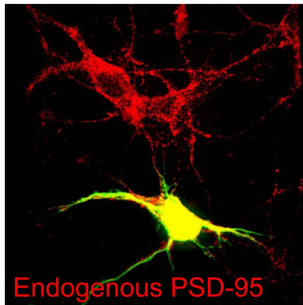


Supplemental file 4 here

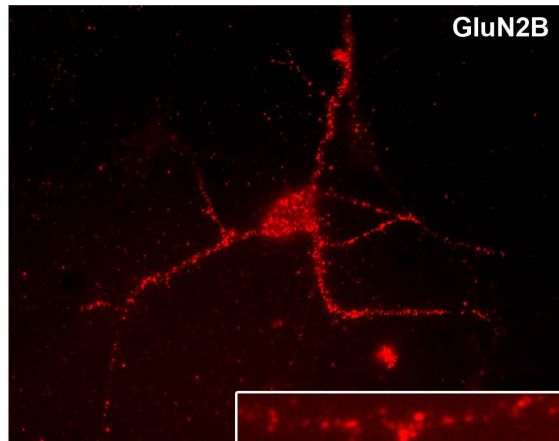
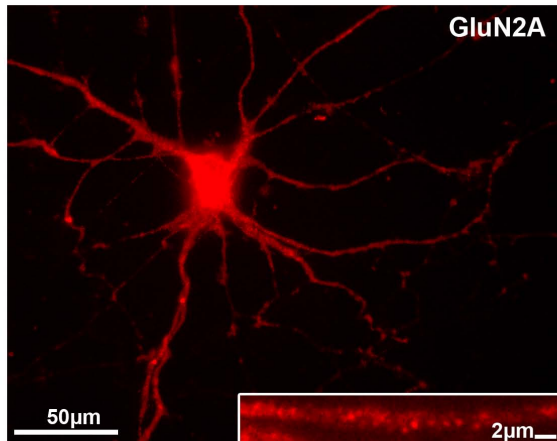




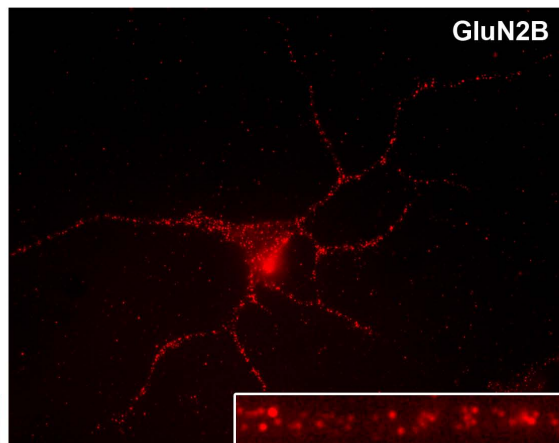
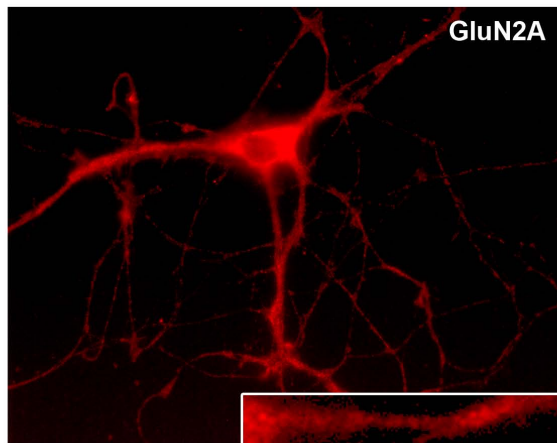
shRNA PSD-95/GFP



vehicle



TAT-D1-CT



TAT-D1-SCR

